Liquid-Crystal Photonic-Band-Gap Materials: The Tunable Electromagnetic Vacuum

Kurt Busch and Sajeev John

Department of Physics, University of Toronto, 60 St. George Street, Toronto, Ontario, Canada M5S 1A7

(Received 2 December 1998)

We demonstrate that when an optically birefringent nematic liquid crystal is infiltrated into the void regions of an inverse opal, photonic-band-gap (PBG) material, the resulting composite material exhibits a completely tunable PBG. In particular, the three-dimensional PBG can be completely opened or closed by applying an electric field which rotates the axis of the nematic molecules relative to the inverse opal backbone. Tunable light localization effects may be realized by controlling the orientational disorder in the nematic.

PACS numbers: 42.70.Qs, 42.70.Df

Photonic-band-gap (PBG) materials are a distinct class of dielectrics which facilitate two fundamentally new optical principles, namely the localization of light [1–5] and the controllable inhibition of spontaneous emission of light from atoms and molecules [6–10]. The utility of PBG materials arises essentially from their ability to realize these two functions. Although an intensive effort has developed over the past ten years [11–13] to microfabricate PBG materials, it is only recently that a clear route to synthesizing large scale three-dimensional PBG materials with submicron lattice constants has been demonstrated [14–16] using self-assembly methods. The application of this approach to Si, Ge, and GaAs based PBG materials may open the door to applications in laser devices and telecommunications as well as to the realization of fundamentally new effects in quantum and nonlinear optics.

For many applications, however, it is advantageous to obtain some degree of tunability of the photonic band structure through electro-optic effects. Such tunability may be obtained by controlling one or several forms of optical anisotropy of the constituent materials. The science of liquid crystals [17–19] has spawned an entire industry related to these electro-optic effects. In earlier works, however, a rather pessimistic conclusion regarding the efficacy of birefringent photonic crystals was drawn [20,21] since attention was restricted to unrealizable structures that consist of spheres of disconnected anisotropic, high dielectric materials in an air background. In other more readily realizable liquid crystal systems [22,23], there was insufficient refractive index contrast to open a three-dimensional PBG. However, it is now well known that inverse opal structures, i.e., air inclusions in a high dielectric backbone material such as silicon provide a much more efficient scattering system both for ordered [15,24] as well as disordered [25] structures. For these inverse opals the optimal filling ratios of the high dielectric backbone lies around 24.5%, leaving a large empty volume for infiltration by a low refractive index liquid crystal with strong optical anisotropy. This large volume of birefringent material makes the resulting composite system highly efficacious for electro-optic tuning effects. In particular, a change in the orientation of the nematic director field with respect to the inverse opal backbone by an external electric field can completely open or close the full, three-dimensional PBG.

In this Letter, we illustrate the principle of the fully tunable electromagnetic vacuum with detailed results on an inverted opal [14,16] made of silicon into which the low index nematic liquid crystal BEHA [19] is infiltrated. For this structure we find that a 2% photonic band gap may be opened or closed, by changing the orientation of the nematic director. In addition, the thermally driven nematic to isotropic liquid phase transition provides further tunability of the PBG. Localized states of light may be created through random fluctuations as well as through singularities (textures) in the nematic director field.

In order to determine the photonic band structure of anisotropic crystals we start with the wave equation satisfied by the magnetic field for a three-dimensional periodic array of scatterers

$$\vec{\nabla} \times [\boldsymbol{\epsilon}^{-1}(\vec{r})\vec{\nabla} \times \vec{H}(\vec{r})] - \frac{\omega^2}{c^2}\vec{H}(\vec{r}) = 0, \quad (1)$$

where $\nabla \cdot \vec{H}(\vec{r}) = 0$. The dielectric tensor $\boldsymbol{\epsilon}(\vec{r} + \vec{R}) = \boldsymbol{\epsilon}(\vec{r})$ is periodic with respect to the set $\mathcal{R} = \{n_1\vec{a}_1 + n_2\vec{a}_2 + n_3\vec{a}_3; (n_1, n_2, n_3) \in \mathcal{Z}^3\}$ of lattice vectors $\vec{R}$ generated by the primitive translations $\vec{a}_i, i = 1, 2, 3$ that describe the structure of the photonic crystal. It may be expanded in a Fourier series on $\mathcal{G}$ the reciprocal (dual) lattice corresponding to $\mathcal{R}$:

$$\boldsymbol{\epsilon}(\vec{r}) = \sum_{\vec{G}\in\mathcal{G}} \boldsymbol{\epsilon}_{\vec{G}} e^{i\vec{G}\vec{r}}. \quad (2)$$

Equation (1) comprises a set of three coupled differential equations with periodic coefficients. Using the Bloch-Flouquet theorem, we may expand the magnetic field as

$$\vec{H}(\vec{r}) \equiv \vec{H}_{\vec{k}}(\vec{r}) = \sum_{\vec{G}\in\mathcal{G}} \sum_{\lambda=1}^{2} h^{\lambda}_{\vec{G}} \hat{e}^{\lambda}_{\vec{G}} e^{i(\vec{k}+\vec{G})\vec{r}}, \quad (3)$$

where λ labels the two transverse polarizations for any plane wave such that $\hat{e}^{\lambda=1,2}_{\vec{G}}$ and $\vec{k} + \vec{G}$ form an orthogonal triad. Because of the discrete translational symmetry of the lattice, the wave vector $\vec{k}$ labeling the solutions may

 © 1999 The American Physical Society

be restricted to lie in the first Brillouin zone (BZ). However, care must be exercised in identifying the irreducible part of the Brilloin zone (IBZ): The dielectric tensor in Eq. (1) may have fewer rotational symmetries than the underlying lattice and consequently, the IBZ for a photonic crystal containing anisotropic materials may be considerably larger than the IBZ for the corresponding isotropic crystal. Rather than dealing with an IBZ that changes from problem to problem, we choose to work with the standard IBZ for the isotropic material and solve Eq. (1) not only for the given form of the dielectric tensor, but also for all inequivalent transformations of it with respect to the rotational symmetries of the underlying lattice.

Consider an optimized inverted opal consisting of a connected high index backbone material such as silicon with total volume fraction of 24.5% [15]. This structure consists of an fcc lattice of close packed air spheres where the space between the spheres has been 90% filled with silicon leaving only tiny air voids between the air spheres. The air spheres themselves are now partially infiltrated with a nematic liquid crystal that wets the interior surface and results in a homogeneous coating (see Fig. 1). The corresponding dielectric tensor is given by

$$\boldsymbol{\epsilon}(\vec{r}\,) = \mathbf{1} + \boldsymbol{\epsilon}_{is} \sum_{\vec{R}\in\mathcal{R}} S_{\rm is}(\vec{r} + \vec{R}) + \boldsymbol{\epsilon}_{\rm LC} \times \sum_{\vec{R}\in\mathcal{R}} S_{\rm LC}(\vec{r} + \vec{R}), \quad (4)$$

where $S_{\rm is}$ and $S_{\rm LC}$ describe the location of the optically isotropic backbone (is) and the liquid crystal (LC) material,

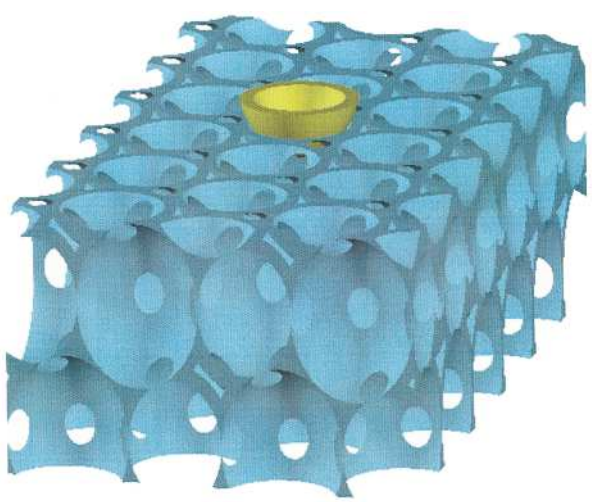

FIG. 1 (color). Cross-sectional view through the inverse opal backbone (blue) resulting from incomplete infiltration of silicon into the air voids of an artificial opal. After etching out the template, a fcc lattice of overlapping air spheres remains and additional air voids appear as triangular or diamond shaped holes on the surface of the cut. A tunable PBG is obtained by infiltrating this backbone with nematic liquid crystal (yellow) which wets the inner surface of *each* sphere (only one is shown in the figure).

respectively, within a Wigner-Seitz cell. $S_{\rm is}(\vec{r}\,)$ is unity if $R_0 \le |\vec{r}\,| \le R_c$ and zero elsewhere while $S_{\rm LC}(\vec{R})$ is unity for $R_i \le |\vec{r}\,| \le R_0$ and zero elsewhere. For the optimized opal $R_0/a = 1/\sqrt{8}$, $R_i/a = 0.2812$, and $R_c/a = 0.445$ where a is the cubic lattice constant of the fcc lattice [15]. The dielectric tensor for silicon is proportional to the unit tensor, i.e., $\boldsymbol{\epsilon}_{\rm is} = (\epsilon_{\rm Si} - 1)\mathbf{1}$ ($\epsilon_{\rm Si} \approx 11.9$). For bulk nematic liquid crystal we may choose a coordinate system in which the dielectric tensor is diagonal with principal entries $\epsilon^{\parallel}_{\rm LC}$ – parallel and $\epsilon^{\perp}_{\rm LC}$ perpendicular to its director $\hat{n}$, respectively. For the inverse opal, the coordinate system is fixed by the high index backbone and the director $\hat{n}$ can have different orientations with respect to this reference frame. Consequently, the dielectric tensor of the nematic takes the form

$$\boldsymbol{\epsilon}_{\rm LC} = \mathbf{O}(\theta,\phi)\,\mathrm{diag}(\epsilon^{\perp}_{\rm LC}, \epsilon^{\perp}_{\rm LC}, \epsilon^{\parallel}_{\rm LC})\mathbf{O}^{T}(\theta,\phi) - 1, \quad (5)$$

where $\mathbf{O}(\theta,\phi)$ is a rotation matrix which acts on the corresponding diagonalized tensor. The angles θ and ϕ describe the orientation of the director n with respect to the inverse opal coordinate system (see Fig. 1). Clearly, the subset of inequivalent rotational transformations (chosen from the larger group of rotational symmetries of the backbone) depends crucially on the orientation of n. As mentioned above, by restricting ourselves to the standard IBZ of the fcc lattice we must compensate by computing the band structures for all distinct dielectric tensors in the set $\mathcal{E} = \{\boldsymbol{\epsilon}^{(s)}_{\rm LC} = \mathbf{S}\boldsymbol{\epsilon}_{\rm LC}\mathbf{S}^{T}, \mathbf{S} \in S\}$. Here S is the lattice point group which in the case of an fcc lattice has 48 elements. This algorithm is equivalent to computing a single band structure throughout the actual IBZ of the birefringent PBG material. As an example, consider the case $\phi = 0$: It is easily checked that for $\theta = 0$ the set $\mathcal{E}$ has three elements whereas for $\theta \neq 0$ the set $\mathcal{E}$ has six elements. In the general case ($\phi \neq 0, \theta \neq 0$) there are twelve inequivalent transformations of $\boldsymbol{\epsilon}_{\rm LC}$ (for $\hat{n} \parallel (1,1,1)$, i.e., $\phi = \pi/4$ and $\theta = \cos^{-1}(1/\sqrt{3})$ the set $\mathcal{E}$ contains only four elements).

Inserting Eqs. (2) and (3) into Eq. (1) results in an infinite matrix eigenvalue problem

$$\sum_{\vec{G}'\in\mathcal{G}} \sum_{\lambda'=1}^{2} \mathbf{M}^{\lambda\lambda'}_{\vec{G}\vec{G}'} h^{\lambda'}_{\vec{G}'} = \frac{\omega^2}{c^2} h^{\lambda}_{\vec{G}}, \quad (6)$$

where the matrix elements $\mathbf{M}^{\lambda\lambda'}_{\vec{G}\vec{G}'}$ are given by

$$\mathbf{M}^{\lambda\lambda'}_{\vec{G}\vec{G}'} = |\vec{k} + \vec{G}|\,(\hat{e}^{\lambda}_{\vec{G}} \cdot \boldsymbol{\epsilon}^{-1}_{\vec{G}-\vec{G}'} \cdot \hat{e}^{\lambda'}_{\vec{G}'})\,|\vec{k} + \vec{G}'|. \quad (7)$$

For numerical purposes Eq. (6) is truncated by retaining only a finite number of reciprocal lattice vectors [15]. In the case of birefringent or biaxial dielectric materials, the dielectric tensor $\boldsymbol{\epsilon}(\vec{r}\,)$ in Eq. (2) is real and symmetric. For materials with inversion symmetry, $\boldsymbol{\epsilon}(\vec{r}\,) = \boldsymbol{\epsilon}(-\vec{r}\,)$, Eq. (6) is likewise a standard real symmetric eigenvalue problem. The main numerical problem in obtaining the eigenvalues from Eq. (6) is the evaluation of the Fourier

coefficients of the inverse dielectric tensor in Eq. (7). As in the case of isotropic dielectric materials [15], this can be done in two different ways: One can calculate the inverse dielectric tensor in real space and then compute its Fourier coefficients. We refer to this as the direct method. Alternatively, one can calculate the matrix of Fourier coefficients of the real space tensor and then take its inverse to obtain the required Fourier coefficients. The latter method was shown by Ho, Chan, and Soukoulis (HCS) [26] to be more efficient than the direct method for the isotropic dielectric tensor. Since both Fourier transformation and matrix inversion are linear operations, for a complete set of plane waves the eigenvalue spectrum obtained by the direct method and for the HCS method must coincide exactly. However, we are numerically restricted to operate on a finite dimensional subspace of the full reciprocal space. This leads to dramatically different rates of convergence of the two methods as the dimension of the subspace (number of plane waves) is increased. Just as in the case of isotropic dielectric materials, for the birefringent PBG, we find that the HCS method converges substantially faster than the direct method. For instance, eigenfrequencies computed with HCS method for 531 and 1219 plane waves, respectively, differ at most by 0.01% of their absolute value, whereas with the direct method the results vary by more than 10%. The results presented below were obtained with HCS method using 531 plane waves.

We now evaluate the tunable band structure of the inverted opal [15], described above, made of silicon. This structure, which consists of about 24.5% silicon by volume, has a 8.6% band gap between bands 8 and 9.

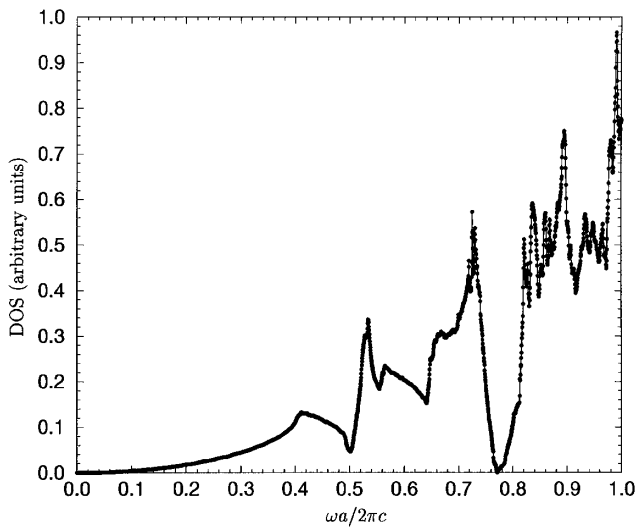

FIG. 2. Total DOS for an inverse opal which is infiltrated with a nematic liquid crystal. The nematic director is orientated along the (0,0,1) axis of the inverse opal backbone. The inverse opal backbone is made of silicon (24.5% by volume) which is infiltrated with the liquid crystal BEHA (36.8% by volume). The isotropic refractive index of silicon is $n_{\mathrm{Si}} = 3.45$ and the principal refractive indices of BEHA are $n_{\mathrm{LC}}^{\parallel} = 1.6$ and $n_{\mathrm{LC}}^{\perp} = 1.4$.

Next, we partially infiltrate the nearly 75% void regions with the nematic liquid crystal BEHA [19] such that it wets the inner surface of the air spheres. The principal indices of refraction for BEHA are $n_{\mathrm{LC}}^{\parallel} = 1.6$ and $n_{\mathrm{LC}}^{\perp} = 1.4$. We choose $R_i = 0.2812a$ so that roughly half the void volume is filled with BEHA and the total volume fraction of BEHA is 36.8%. In Fig. 2 we show the total photon density of states (DOS) when the nematic director $\hat{n}$ is oriented along the (0,0,1) axis of the fcc backbone. The complete 8.6% photonic band gap of the inverse opal backbone is destroyed upon infiltration of the liquid crystal but a pronounced pseudogap with a low DOS remains. The closing of the band gap between bands 8 and 9 for $\hat{n} = (0, 0, 1)$ occurs first at the W points of the full Brillouin zone which experience a strong anisotropy. If $\hat{n}$ is rotated away from the (0,0,1) direction, different high symmetry points in the Brillouin zone will be affected differently. Most notably, the anisotropy seen by the W points will be reduced. In Fig. 3 we display the dependence of the gap size between bands 8 and 9 as $\hat{n}$ rotates from (0,0,1) through (1,1,1) to the (1,1,0) direction. In terms of spherical coordinates, $\phi = \pi/4$ and θ ranges from 0 to $\pi/2$. For the liquid crystal PBG material, this leads to an opening of a complete photonic band gap. The PBG reaches a maximum value of 1.6%, when $\hat{n}$ points along the (1,1,1) axis, direction for which the anisotropy as seen by the W point is at a minimum. The effect of reorienting $\hat{n}$ on the photon density of states is further illustrated in Fig. 4, where, for fixed $\phi = \pi/4$, we consider various values of the angle θ. This clearly demonstrates an electro-optic shutter effect to the complete three-dimensional photonic band gap which may be realized by an external electric field that controls the orientation of the nematic molecules.

As stated in the introduction, the utility of PBG materials arises from the two fundamental optical principles

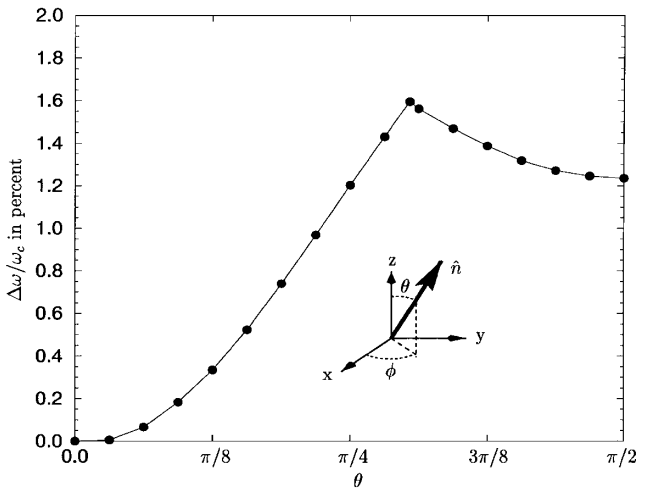

FIG. 3. Dependence of the photonic-band-gap size for a silicon inverted opal infiltrated with the nematic liquid crystal (BEHA) on the orientation of the nematic director $\hat{n}(\phi, \theta)$ for fixed angle $\phi = \pi/4$. The volume fractions are the same as in Fig. 2.

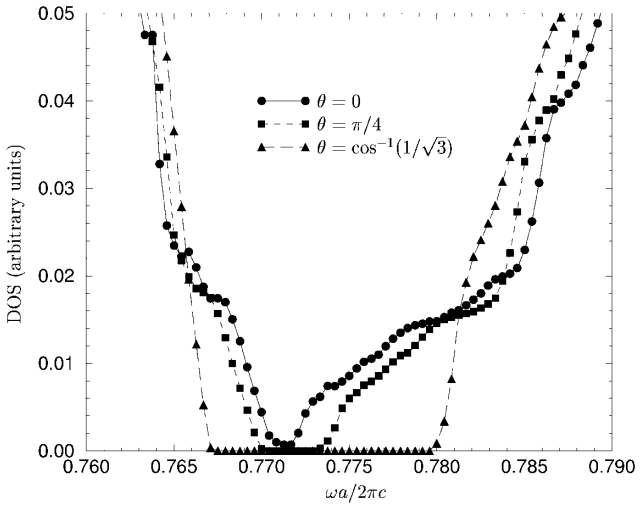

FIG. 4. Total photon DOS for a silicon inverse opal which is infiltrated with the nematic liquid crystal (BEHA) for various orientations of the nematic director $\hat{n}(\phi, \theta)$. The angle $\phi = \pi/4$ is fixed and the volume fractions are the same as in Fig. 2. The PBG is closed for $\theta = 0$, but reaches a maximum value $\Delta\omega/\omega_c \simeq 1.6\%$ relative to its center frequency ω_c for $\hat{n} = (1, 1, 1)/\sqrt{3}$.

which they facilitate: (i) The localization of light and (ii) the control of spontaneous emission. The tunable liquid crystal PBG material may facilitate electro-optic modulation of laser light emission along the W direction from active molecules placed within the material. It will also facilitate an electro-optical tuning of the propagation and localization of light in the vicinity of the gap. For a thermally disordered nematic liquid crystal, a dramatic modification of the Ioffe-Regel criterion [27] for localization may be realized. Light localization in a disordered dielectric medium is expected [1,2,28] when

$$\pi^2 c\rho(\omega)(\ell^*)^2 \simeq 1\,. \tag{8}$$

Here, c is the speed of light in vacuum, $\rho(\omega)$ is the photon density of states at frequency ω, and ℓ^* is the transport mean free path for photons, determined by the extent of disorder in the medium. For photons in ordinary vacuum ($\omega = ck$), $\rho(\omega) = \omega^2/(\pi^2 c^3)$ and this condition reduces to the Ioffe-Regel condition, $\ell^*(\omega/c) \simeq 1$. However, in the liquid crystal PBG material, ℓ^* represents the transport mean free path for optical Bloch waves arising from the deviations of the medium from perfect periodicity. The very low DOS (depending on the orientation of $\hat{n}$) at the bottom of the pseudogap or near the complete band gap, provides a very favorable scenario for the photon localization according to criterion (8) even when $\ell^*(\omega/c) \gg 1$. For a nematic which is well ordered and fully aligned in the (1,1,1) direction, tunable waveguiding effects may be realized by locally applying an electric field which reorients the nematic director field along the (1,0,0) direction along specific channels that pass through the PBG material. The resulting tunability of spontaneous emission, waveguiding effects, and light localization may considerably enhance the technological utility of liquid crystal photonic band gap materials over and above that of either a bulk liquid crystal or a conventional photonic crystal by itself.

We are grateful to Professor Katsumi Yoshino for stimulating discussions concerning the experimental realization of the liquid crystal inverse opal structure. This work was supported in part by the New Energy and Industrial Technology Development Organization of Japan and by Photonics Research Ontario. K. B. would like to acknowledge the financial support by the Deutsche Forschungsgemeinschaft (DFG) under Grant No. Bu 1107/1-1.

[1] S. John, Phys. Rev. Lett. **53**, 2169 (1984).
[2] S. John, Phys. Rev. Lett. **58**, 2486 (1987).
[3] P. W. Anderson, Philos. Mag. B **52**, 505 (1985).
[4] A. Z. Genack and N. Garcia, Phys. Rev. Lett. **66**, 2064 (1991).
[5] D. Wiersma *et al.,* Nature (London) **390**, 671 (1997).
[6] V. P. Bykov, Sov. J. Quantum Electron. **4**, 861 (1975).
[7] E. Yablonovitch, Phys. Rev. Lett. **58**, 2059 (1987).
[8] S. John and J. Wang, Phys. Rev. Lett. **64**, 2418 (1990).
[9] S. John and T. Quang, Phys. Rev. A **50**, 1764 (1994).
[10] T. Quang *et al.,* Phys. Rev. Lett. **79**, 5238 (1997).
[11] For a recent review on photonic crystal research and its applications, we refer to *Photonic Band Gap Materials,* edited by C. M. Soukoulis (Kluwer Academic, Dordrecht, 1996).
[12] S. Lin *et al.,* Nature (London) **394**, 251 (1998).
[13] N. Yamamoto, S. Noda, and A. Chutinan, Jpn. J. Appl. Phys. **37**, L1052 (1998).
[14] J. E. G. J. Wijnhoven and W. L. Vos, Science **281**, 802 (1998).
[15] K. Busch and S. John, Phys. Rev. E **58**, 3896 (1998).
[16] A. A. Zakhidov *et al.,* Science **282**, 897 (1998).
[17] P. G. de Gennes and J. Prost, *The Physics of Liquid Crystals* (Clarendon Press, Oxford, England, 1993).
[18] S. Chandrasekhar, *Liquid Crystals* (Cambridge University Press, Cambridge, England, 1992).
[19] L. M. Blinov and V. G. Chigrinov, *Electro-Optic Effects in Liquid Crystal Materials* (Springer, New York, 1994).
[20] I. H. H. Zabel and D. Stroud, Phys. Rev. B **48**, 5004 (1993).
[21] Z.-Y. Li, J. Wang, and B.-Y. Gu, Phys. Rev. B **58**, 3721 (1998).
[22] R. M. Hornreich, S. Shtrikman, and C. Sommers, Phys. Rev. E **47**, 2067 (1993).
[23] V. I. Kopp, B. Fan, H. K. M. Vithana, and A. Z. Genack, Opt. Lett. **23**, 1707 (1998).
[24] H. S. Sözuer, J. W. Haus, and R. Inguva, Phys. Rev. B **45**, 13 962 (1992).
[25] K. Busch and C. M. Soukoulis, Phys. Rev. Lett. **75**, 3442 (1995).
[26] K.-M. Ho, C. T. Chan, and C. M. Soukoulis, Phys. Rev. Lett. **65**, 3152 (1990).
[27] A. I. Ioffe and A. R. Regel, Prog. Semicond. **4**, 237 (1960).
[28] S. John and R. Rangarajan, Phys. Rev. B **38**, 10 101 (1988).